Low-Energy Cs^+ Scattering from Water on Pt(111): A Kinetic Energy Analysis of the Cs^+−Water Clusters†

J. R. Hahn,‡ C. W. Lee,§ S.-J. Han,§,|| R. J. W. E. Lahaye,‡ and H. Kang*,‡

School of Chemistry, Seoul National University, Kwanak-ku, Seoul 151-742, South Korea, and Department of Chemistry, Pohang University of Science and Technology, Pohang 790-784, South Korea

Received: February 6, 2002; In Final Form: May 15, 2002

We measured the kinetic energy of Cs^+ and $Cs(H_2O)_n^+$ ($n = 1-3$) cluster ions formed in reactive scattering of low-energy (20−80 eV) Cs^+ from physisorbed water on Pt(111). Reflected Cs^+ primaries show two components in the energy spectrum: one scattered from surface water molecules appearing at low energy and another from bare Pt atoms at a higher energy. The former is efficiently converted to $Cs(H_2O)_n^+$, the reaction probability being close to unity at full coverage with water. The kinetic energies of the clusters are presented as a function of incident beam energy, scattering angle, and water exposure. On the basis of these results, we propose a cluster formation mechanism in which slow Cs^+ picks up water molecules via an ion-surface abstraction reaction. At high energy, Cs^+ penetrates into a physisorbed layer and the clustering reactions may also take place inside the collisionally activated volume of the layer.

Introduction

Reactive scattering of low-energy (1−100 eV) ion projectiles at surfaces, often called reactive ion scattering (RIS), has gained considerable attention over the past decade. Whereas conventional ion scattering spectrometry uses the elastic scattering of noble gas or alkali metal ion projectiles, the use of chemically active projectiles opens a variety of reactive channels in the scattering process. RIS adds rich chemistry to the physics of ion scattering. Among the many interesting RIS phenomena discovered to date,[1−16] the scattering process that involves transfer of an atom or molecule between a projectile and a surface is of particular interest, which has potential application for surface modification and analysis. Rabalais and co-workers[6] observed that low-energy C^+ ions incident on O/Ni(111) efficiently deplete surface O atoms, suggesting that C^+ picks up an O atom and scatters as CO. Cooks and co-workers[2−4] discovered a variety of exchange processes of atoms or functional groups in experiments employing polyatomic ion projectiles and self-assembled monolayers. Wu and Hanley[7] reported the pickup of H by pyridine ions. More recently, Jacobs and co-workers reported the abstraction of O atoms by O^+ at an oxidized Si(100) surface[8] and by NO^+ at O/Al(111).[9] In these studies, the kinetic energy and the angular distribution of scattered ions have provided valuable information on the mechanisms of RIS.[2−5,8−11]

In an earlier study,[12] we reported that low-energy Cs^+ can pick up water molecules chemisorbed on Si(111) and scatters as CsH_2O^+. This phenomenon, called Cs^+ RIS, has since been examined with a variety of surfaces, demonstrating that it can be applied to the analysis of surface molecules.[13] It has been suggested[12] that Cs^+ RIS occurs in a two-step mechanism: the desorption of surface water molecules by ion impact (reaction 1) and the association reaction between the desorbed water and the scattered Cs^+ in gas phase near the surface (reaction 2):

$$Cs^+(g) + H_2O(s) \rightarrow Cs^+(g) + H_2O(g) \quad (1)$$

$$Cs^+(g) + H_2O(g) \rightarrow [CsH_2O^+(g)]' \rightarrow CsH_2O^+(g) \quad (2)$$

$[CsH_2O^+(g)]'$ denotes a transient complex formed by Cs^+ and H_2O association, which is stabilized to $CsH_2O^+(g)$ by energy loss, for instance, to the surface. The yield for RIS (Y_{ris}), which is defined by the number of cluster ions formed per incident Cs^+, is $10^{-3}-10^{-4}$ for typical chemisorbed molecules.[12,13] On the other hand, drastically different behavior has been observed for Cs^+ RIS on physisorbed surfaces.[14−16] On a frozen water layer prepared on low-temperature Si(111),[14] Y_{ris} is increased by 10^2-10^3 times compared to that from chemisorbed water. In addition, Cs^+ can pick up more than one water molecule, producing multihydrated clusters $Cs(H_2O)_n^+$ with $n > 1$. This suggests that the nature of the scattering process is greatly changed on a physisorbed layer, but its explanation is unclear. In the present study, we have taken a step further in exploring the RIS process at a physisorbed layer. We chose Pt(111) as a substrate for depositing water, on which water is known[17] to adsorb in an ordered $(\sqrt{3} \times \sqrt{3})R30°$ phase and form an icelike structure; this water layer is better characterized than that formed on Si(111). Kinetic energy was analyzed for the scattered Cs^+ and $Cs(H_2O)_n^+$ ions as a function of water exposure, incident beam energy, and scattering angle. These results led us to propose plausible mechanisms for the RIS process.

Experimental Section

Experiments were carried out in an RIS chamber maintained at a base pressure of 5×10^{-11} Torr.[18] A Pt(111) sample was cleaned by repeated cycles of 2 keV Ar^+ sputtering at 800 K, oxidation in O_2 environment at 700 K, and annealing at 1200 K in UHV. The surface cleanness was checked by Auger

† Part of the special issue "Jack Beauchamp Festschrift".

* Corresponding author: e-mail surfion@snu.ac.kr; fax +82 2 889 8156.
‡ School of Chemistry, Seoul National University.
§ Department of Chemistry, Pohang University of Science and Technology.
|| Present address: Department of Physics, Pohang University of Science and Technology, Pohang 790-784, South Korea.

10.1021/jp0203402 CCC: $22.00
Published on Web 07/02/2002

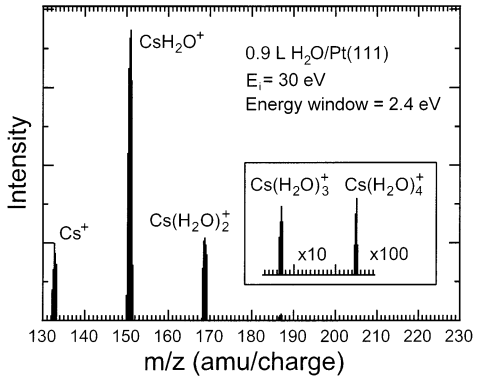

Figure 1. Mass spectrum of positive ions generated by Cs^+ RIS from a frozen water layer on Pt(111) at 110 K. H_2O exposure on the surface was 0.9 L. In the inset, intensities of larger clusters are magnified by the factors indicated. E_i was 30 eV, and incidence and exit angles both were 45°. The transmission energy window for scattered ions was 2.4 ± 0.2 eV.

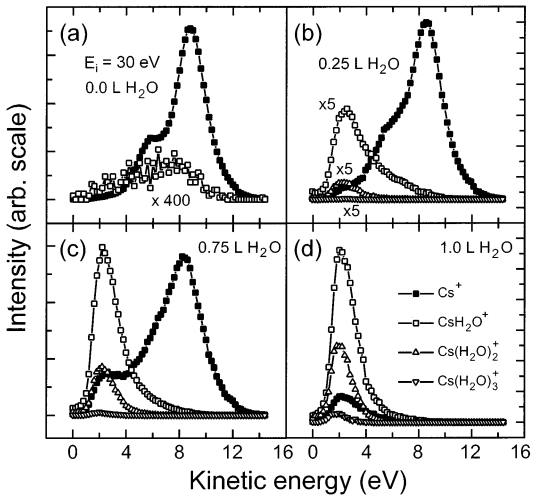

Figure 2. Kinetic energy spectra of scattered ions as a function of H_2O exposure at 110 K. (a) Clean Pt(111) surface; (b) H_2O exposure = 0.25 L, (c) 0.75 L, and (d) 1.0 L. E_i was 30 eV, and incidence and exit angles both were 45°.

electron spectroscopy and Cs^+ RIS. Water was exposed to Pt(111) at a temperature of 110 K by back-filling the chamber at an H_2O pressure of 5×10^{-9} Torr. H_2O is known[17] to physisorb in a layer-by-layer fashion on Pt(111) under this condition. The doser was also away from an ionization gauge in order to minimize the error in reading the H_2O pressure.

The angle- and energy-resolved RIS apparatus has been described in detail elsewhere.[18] Briefly, Cs^+ ions produced from a surface ionization source were scattered at a target surface at the desired collision energy between 20 and 80 eV. The Cs^+ current density at the target was 0.5−5 nA/cm^2. Ions scattered from the surface were analyzed for mass by a QMS (ABB Extrel) with the ionizer off. Kinetic energy of the scattered ions was analyzed by an axial energy analyzer (a Bessel filter) located in front of a quadrupole mass filter. For kinetic energy measurement, we fixed the quadrupole filter to selectively transmit ions of a particular mass-to-charge ratio and scanned the energy analyzer. Holding the energy analyzer fixed while scanning the quadrupole filter yielded a mass spectrum of ions with a particular kinetic energy window. The energy analyzer was calibrated by directing a Cs^+ beam to the analyzer axis, and the energy resolution was set at 0.3 eV unless specified otherwise. Angle-resolved scattering experiments were done by independently rotating the Cs^+ gun and the sample in a scattering plane defined by the gun, sample, and QMS detector.

Results

A mass spectrum of Cs^+ RIS products scattered from a Pt(111) surface physisorbed with water is shown in Figure 1. The sample was exposed to H_2O vapor for 0.9 L (1 L = 1×10^{-6} Torr s) at 110 K. The energy of the incident Cs^+ beam (E_i) was 30 eV, and ion incidence and exit angles both were 45° to the surface. The transmission energy window for scattered ions was 2.4 ± 0.2 eV. The mass spectrum shows a series of hydrated cluster ions, $Cs(H_2O)_n^+$ with $n = 1-4$, together with reflected Cs^+ primaries. The mass identification of clusters was verified by the isotopic shifts on a D_2O-adsorbed surface.[14−16] The strongest peak seen is CsH_2O^+, which is even stronger than Cs^+. The intensity of $Cs(H_2O)_n^+$ decreases with an increase of n. In the mass region below 130 amu/charge, no secondary ions were detected.

Figure 2 shows the kinetic energy distributions of scattered Cs^+ and $Cs(H_2O)_n^+$ measured for different H_2O coverages. The energy spectra were obtained with energy increments of 0.2 eV. Incident beam energy and scattering angle were the same as in Figure 1. On clean Pt(111) [Figure 2a], the Cs^+ energy spectrum exhibits two peaks at 5.8 and 8.9 eV. The energies of 5.8 and 8.9 eV correspond to energy transfer efficiencies of 81% and 70%, respectively, from incident Cs^+ to the surface. We interpret that the two peaks are due to scattering from different impact sites in the unit cell of the Pt(111) surface, by comparing the energy transfer efficiencies with the result of molecular dynamics (MD) trajectory simulations.[19] The low-energy peak results from impacts around the Pt atop site, and the high-energy peak is due to impacts along the bridge site and around the center site. Figure 2a also shows a spectrum of CsH_2O^+ due to adsorption of residual H_2O vapor, with its intensity magnified by a factor of 400. The presence of residual H_2O in small amounts did not noticeably change the energy spectrum of scattered Cs^+.

In Figure 2b−d, the surface was exposed to increasing amounts of H_2O (0.25, 0.75, and 1.0 L) at 110 K. First, notice that the Cs^+ peaks at 5.8 and 8.9 eV decrease in intensity with increasing water exposure and eventually disappear at 1 L exposure. The two peaks become also somewhat broadened. These changes must be due to the formation of a water layer on the surface. Second, a new peak appears in a Cs^+ energy spectrum at 2 eV. This peak corresponds to an energy transfer efficiency of 93% from Cs^+ to the surface, which suggests that Cs^+ scatters from H_2O molecules. Third, $Cs(H_2O)_n^+$ clusters ($n = 1-3$) have an energy distribution peak near 2 eV, similar to the energy of Cs^+ scattered from H_2O. The peak position of the cluster energy distributions, however, shifts slightly to lower energy with increasing H_2O exposure. At a fixed H_2O coverage, the peak energy is slightly different for different clusters, which is in the order $CsH_2O^+ > Cs(H_2O)_2^+ > Cs(H_2O)_3^+$.

Figure 3 presents the relative yield of scattered Cs^+ and $Cs(H_2O)_n^+$ as a function of water exposure. To calculate the relative yield, the intensity of each species was obtained by integration of its energy spectrum and then normalized to the sum of all intensities. Two components of scattered Cs^+ are separately presented in the plot: Cs^+ scattered from Pt (Cs^+_{Pt}) and Cs^+ scattered from water (Cs^+_{water}), as they are deconvoluted from the Cs^+ energy spectrum. The intensity of Cs^+_{Pt} steadily decreases with an increase in water exposure and drops to almost zero above 1.0 L. This indicates that above 1.0 L exposure, all Pt sites are effectively covered by water molecules. Since water physisorbs on Pt(111) in a layer-by-layer fashion

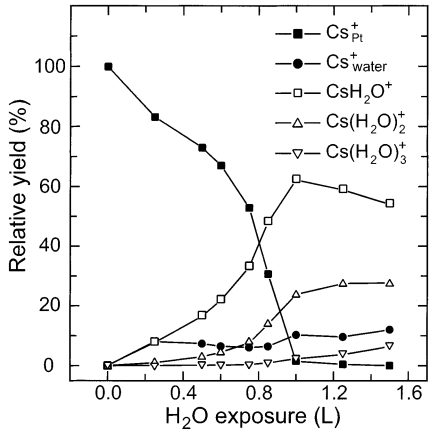

Figure 3. Variation of the relative yield for Cs^+_{Pt}, Cs^+_{water}, CsH_2O^+, $Cs(H_2O)_2^+$, and $Cs(H_2O)_3^+$ as a function of H_2O exposure. Cs^+_{Pt} and Cs^+_{water} indicate Cs^+ ions scattered from clean Pt(111) and water, respectively. E_i was 30 eV, and incidence and exit angles were 45°.

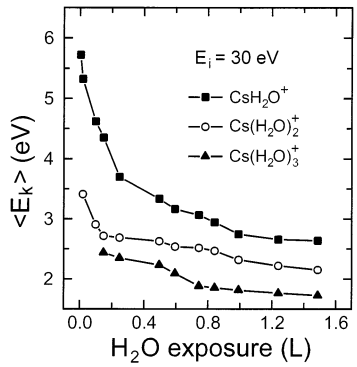

Figure 4. Average kinetic energy, $\langle E_k \rangle$, of $Cs(H_2O)_n^+$ ($n = 1-3$) as a function of H_2O exposure. Ion incidence and exit angles both were 45°.

to form an icelike structure,[17] the water layer formed at this exposure is considered to have a monolayer thickness. It is not clear, however, whether the layer corresponds to one "bilayer" of the ice structure or just a "first layer" of water molecules of the bilayer (the latter denotes H_2O molecules directly bound to Pt with O end down). At water exposures greater than 1.0 L, the relative yield for CsH_2O^+ somewhat decreases, unlike the yields for $Cs(H_2O)_2^+$ and $Cs(H_2O)_3^+$, which still increase. Such variations indicate that multihydrated clusters are more efficiently formed at higher water coverage, although the measurement was made at a fixed scattering angle. The vast majority of incident Cs^+ ions form hydrated clusters above 1.0 L, and the reflected Cs^+ has a very small intensity. Y_{ris} reaches 0.9 in this regime.

The kinetic energy of clusters was examined as a function of water exposure (Figure 4), incident beam energy (Figure 5), and scattering angle (Figure 6). The results are presented with respect to the average value of the kinetic energy distribution ($\langle E_k \rangle$). Figure 4 shows the variation in $\langle E_k \rangle$ of $Cs(H_2O)_n^+$ ($n = 1-3$) for water exposures of 0.0−1.5 L. E_i was 30 eV, and the scattering geometry was 45°/45°. The kinetic energy of clusters continuously decreases with an increase in water exposure. This indicates that Cs^+ transfers more energy to a surface in cluster formation at higher water coverage. At low coverages, the kinetic energy decreases more rapidly for CsH_2O^+ than for multihydrated clusters. This trend results from the disappearance of a high-energy tail in the CsH_2O^+ energy spectrum, as can be seen in Figure 2.

Figure 5 panels a and b present cluster energy distributions measured at $E_i = 20$ and 80 eV, respectively. Variation of $\langle E_k \rangle$

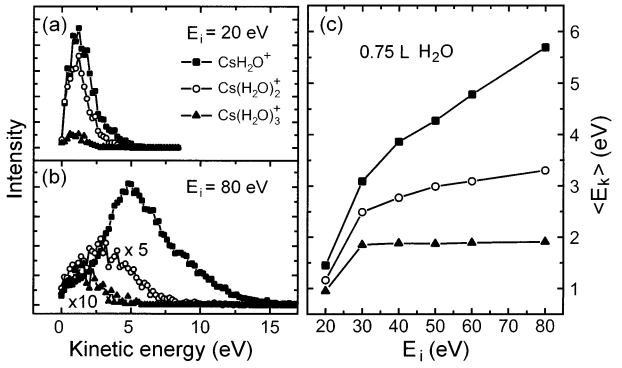

Figure 5. Energy spectra of $Cs(H_2O)_n^+$ ($n = 1-3$) at $E_i = 20$ eV (a) and 80 eV (b). Variation of the average kinetic energy $\langle E_k \rangle$ as a function of E_i is shown in panel c. The intensities of $Cs(H_2O)_2^+$ and $Cs(H_2O)_3^+$ in panel b are amplified by the factors indicated. Incidence and exit angles both were 45°, and H_2O exposure was 0.75 L.

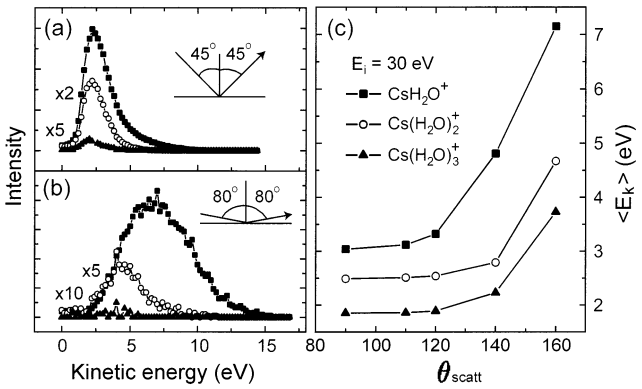

Figure 6. Energy spectra of $Cs(H_2O)_n^+$ ($n = 1-3$) at a total scattering angle, θ_{scatt}, of 90° (a) and 160° (b). $\theta_{scatt} = \theta_i + \theta_f$, with θ_i and θ_f defined as shown in the figure. Variation of $\langle E_k \rangle$ as a function of θ_{scatt} is shown in panel c. The intensities of $Cs(H_2O)_2^+$ and $Cs(H_2O)_3^+$ in panels a and b are amplified by the factors indicated. E_i was 30 eV, and H_2O exposure was 0.75 L.

with E_i is plotted in Figure 5c for the range of 20−80 eV. Water exposure was fixed at 0.75 L. The kinetic energy of CsH_2O^+ increases continuously with E_i, but for $Cs(H_2O)_3^+$ it stays fairly constant for $E_i > 30$ eV; $Cs(H_2O)_2^+$ exhibits intermediate behavior. In Figure 5a, the energy spectra at 20 eV are relatively narrow and overlap for clusters of different sizes. At 80 eV (Figure 5b), on the other hand, the spectrum of CsH_2O^+ is broad, shifted distinctly to a higher energy, and has a much larger intensity than the other clusters.

The effect of scattering angle on the energy distribution of clusters is examined in Figure 6. Figure 6a shows the energy distributions measured at a total scattering angle, θ_{scatt}, of 90° in specular geometry, in which incidence (θ_i) and exit angles (θ_f) both are 45° with respect to the surface normal. Figure 6b shows the result for $\theta_{scatt} = 160°$ ($\theta_i = \theta_f = 80°$). At larger θ_{scatt}, the energy distribution shifts to a higher energy and the relative yield of CsH_2O^+ increases. Variation of $\langle E_k \rangle$ with θ_{scatt} is presented in Figure 6c, which reveals a reduced energy transfer to the surface with increasing θ_{scatt}.

Discussion

The present study shows several unique features for Cs^+ RIS on a physisorbed water layer, which can be reiterated as follows. The RIS yield is orders of magnitude higher than that for chemisorbed molecules; it is close to unity at full coverage of water on the surface. Multihydrated clusters are efficiently formed. Kinetic energy of clusters is very low, and the clusters

of different sizes overlap in energy with each other, as well as with Cs^+_{water}. The kinetic energy for $Cs(H_2O)_n^+$ decreases with the increase of n, but the decrease is marginal at low E_i, whereas it becomes more distinct at higher E_i. The kinetic energy decreases with an increase in water exposure and also with an increase in scattering angle. In the following, we discuss the possible mechanisms of cluster formation in the light of these observations.

In an earlier study,[14] two mechanistic models have been proposed for $Cs(H_2O)_n^+$ formation from a frozen water layer. One is the successive pickup of water molecules by Cs^+, which is denoted as model I. In this mechanism, $Cs(H_2O)_n^+$ grows through sequential association reactions between Cs^+ and H_2O, similar to the clustering reactions in a supersonic nozzle expansion of gases (reactions 3 and 4):

$$Cs^+(g) + H_2O(g) \rightarrow CsH_2O^+(g) \quad (3)$$

$$Cs(H_2O)_{n-1}^+(g) + H_2O(g) \rightarrow Cs(H_2O)_n^+(g) \quad (4)$$

To account for the high Y_{ris} value of the cluster formation, it has been proposed that the clusters are created under a condition of extremely high H_2O density, i.e., in a quasi-condensed phase, in contrast to the gas-phase Cs^+-H_2O association reaction in the two-step RIS process (reactions 1 and 2). That is, Cs^+ penetrates into a frozen water layer and the clustering reactions occur inside the collisionally activated region of the layer. The idea of surface penetration has been supported by the observation that the scattered Cs^+ intensity decreases as the thickness of a frozen water layer on Si(111) increases.[14]

An alternative model (model II) has also been proposed.[14] In this model, multiply hydrated clusters are initially ejected from the surface upon Cs^+ impact. The clusters are formed with high internal excitation and as such, they are cooled by unimolecularly fragmenting in the gas phase, producing smaller clusters:

$$Cs^+(g) + H_2O(s) \rightarrow [Cs(H_2O)_n^+(g)]' \rightarrow Cs(H_2O)_m^+(g) + (n-m)H_2O(g) \quad (5)$$

where $m < n$.

According to model I, the kinetic energy of a cluster is expected to decrease with an increase in cluster size, since a cluster grows through sequential momentum-transfer collisions with water molecules. Collisions in a condensed phase will significantly reduce the kinetic energy of a projectile, and thus the cluster kinetic energy will scale down somewhat linearly with the number of hydrated water molecules. This expectation agrees with the cluster energies measured at $E_i = 80$ eV (Figure 5b). There are, however, several lines of evidence against this model. At 20 eV, the experimental kinetic energy is similar for all clusters or only slightly decreased for the larger clusters, which are produced still in high abundance (Figure 5a). In an RIS study performed on an ice film that is composed of alternate H_2O and D_2O monolayers deposited on Ru(001),[20] the penetration depth of Cs^+ was found to be at most one water layer at $E_i = 10$ eV. The penetration depth exceeded one layer at 40 eV. Therefore, the cluster formation inside a water film seems unlikely at low E_i. These observations suggest that the clusters formed in the low-E_i regime are not due to surface penetration of Cs^+ and multiple collisions inside a water layer.

In model II, unimolecular dissociation of multihydrated clusters in a gas phase will produce daughter clusters that have the same mean velocity as the parent clusters. The kinetic energy in this case will increase in proportion to the mass of a cluster, such that CsH_2O^+, $Cs(H_2O)_2^+$, and $Cs(H_2O)_3^+$ have a kinetic energy ratio of 1.00:1.12:1.24. The experimental kinetic energies, however, exhibit an opposite trend. In addition, it is not clear how the large clusters can be formed by low-energy Cs^+ impact in the first place.

Therefore, it seems evident that neither model I nor II is satisfactory for explaining the cluster formation. An adequate model must be able to explain the large Y_{ris} value and the clusters' kinetic energies without invoking collisions in a condensed phase. In MD simulations of Cs^+ RIS with physisorbed molecules,[21] we found that weakly adsorbed molecules can be picked up efficiently by Cs^+ via an ion-surface abstraction reaction, even when the impact-induced desorption of molecules does not occur. The abstraction reaction prevails when the binding energy between Cs^+ and the adsorbate is greater than the binding energy of the adsorbate with the surface, a condition that can be met in many physisorption systems, including water on Pt. In this process, the incoming Cs^+ does not hit the adsorbate directly but drags it along the outgoing trajectory *after* the Cs^+ collided with the surface, resulting in an abstraction reaction of an Eley−Rideal type. An important criterion for the cluster formation is that the outgoing Cs^+ must be slow enough to accommodate the inertia of the adsorbate. This explains why the $Cs(H_2O)_n^+$ cluster energy shows no or only minor dependence on the incident energy of Cs^+; only the slow ions in an energy spectrum of scattered Cs^+ form clusters regardless of the incident energy. Moreover, since the inertia increases with mass, the kinetic energy of clusters should decrease with mass. In addition, it should be possible for Cs^+ to abstract more than just one water molecule from the surface, either at once or in a successive manner, forming multihydrated clusters without penetration into a water layer. These features are consistent with the cluster kinetic energies observed at $E_i = 20$ eV (Figure 5a). At grazing angles the kinetic energy of the scattered Cs^+ is higher. This increases the average cluster energy but also decreases the formation yield because the efficiency of abstraction reaction is reduced. Both effects are seen in the cluster energy distributions in Figure 6.

At high incident energy, Cs^+ can penetrate into a frozen water surface, causing damage and collisional cascades of water molecules in the layer. The clustering reactions taking place with water molecules under such an activated environment may be described more adequately by model I. The transition from the abstraction reaction mechanism to this one is reflected by the strong influence of E_i on the energy of CsH_2O^+ (Figure 5c). Nevertheless, the larger clusters [$Cs(H_2O)_2^+$ and $Cs(H_2O)_3^+$] show the rather weak E_i dependence even at high energy, suggesting that they are formed preferentially through the abstraction reaction. At high incident energy the ion impact reduces the water desorption energy by breaking interwater hydrogen bonds, which in turn will enhance the abstraction reaction. Once a large cluster is formed, it may be unimolecularly fragmented on its outgoing trajectory with a certain probability depending on internal energy (model II). The experimental energy spectra, however, reveals no sign of this effect, implying that the fragmentation is minor if it occurs at all.

Conclusions

$Cs(H_2O)_n^+$ clusters are efficiently formed during the reactive scattering of low-energy Cs^+ from a physisorbed water layer on Pt(111). To elucidate the cluster formation mechanism, we

examined the kinetic energy of scattered ions under various experimental conditions, from which the following conclusions have been drawn.

(i) Cs^+ scattered from bare Pt atoms (Cs^+_{Pt}) and from surface water molecules (Cs^+_{water}) are well distinguished in a kinetic energy spectrum. Cs^+_{Pt} has two energy components reflecting different impact sites on the Pt(111) surface. Cs^+_{water} has very low energy, similar to $Cs(H_2O)_n^+$ clusters, and therefore is efficiently converted to the clusters. Y_{ris} for cluster formation is near unity on a water-saturated Pt surface.

(ii) Clusters of different masses overlap largely in their kinetic energy distribution. The average kinetic energy of clusters $\langle E_k \rangle$ slightly decreases with an increase of cluster mass for low E_i, whereas the decrease is greater at higher E_i. $\langle E_k \rangle$ decreases with an increase in water exposure and with a decrease in scattering angle.

(iii) Two mechanisms are proposed for cluster formation observed in the present E_i range. At low E_i, Cs^+ picks up water molecules via an Eley-Rideal type abstraction reaction. Collisional desorption of water molecules is not necessary in this case. At high E_i, Cs^+ penetrates into a frozen water surface, and clustering reactions may take place in a collisionally activated, condensed phase. The abstraction reaction mechanism may still be dominant to form higher order clusters.

Acknowledgment. This work was supported by the BK21 Program of the Ministry of Education, Republic of Korea. H.K. acknowledges Professor Jack Beauchamp, to whom this volume is dedicated, and who suggested a superb idea of scattering reactive ions at a frozen water surface about 20 years ago while serving as the author's graduate advisor. After so many years, it is a great pleasure to emphasize in this work that the idea was correct.

References and Notes

(1) Kasi, S. R.; Kang, H.; Sass, C. S.; Rabalais, J. W. *Surf. Sci. Rep.* **1989**, *10*, 1.

(2) Cooks, R. G.; Ast, T.; Mabud, M. A. *Int. J. Mass Spectrom. Ion Processes* **1990**, *100*, 209.

(3) Morris, M. R.; Riederer, D. E.; Winger, B. E., Jr.; Cooks, R. G.; Ast, T.; Chidsey, C. E. D. *Int. J. Mass Spectrom. Ion Processes* **1992**, *122*, 181.

(4) Cooks, R. G.; Ast, T.; Pradeep, T.; Wysocki, V. *Acc. Chem. Res.* **1994**, *27*, 316, and references therein.

(5) Murata, Y. *Unimolecular and Bimolecular Reaction Dynamics*; Ng, C. Y., Baer, T., Powis, T., Eds.; John Wiley & Sons: New York, 1994; Chapter 9.

(6) Kang, H.; Kasi, S. R.; Grizzi, O.; Rabalais, J. W. *J. Chem. Phys.* **1988**, *88*, 5894.

(7) Wu, Q.; Hanley, L. *J. Phys. Chem.* **1993**, *97*, 2677.

(8) Quinteros, C. L.; Tzvetkov, T.; Jacobs, D. C. *J. Chem. Phys.* **2000**, *113*, 5119.

(9) Maazouz, M.; Barstis, T. L. O.; Maazouz, P. L.; Jacobs, D. C. *Phys. Rev. Lett.* **2000**, *84*, 1331.

(10) Koppers, W. R.; Beijersbergen, J. H. M.; Weeding, T. L.; Kistemaker, P. G.; Kleyn, A. W. *J. Chem. Phys.* **1997**, *107*, 10736.

(11) Schultz, D. G.; Hanley, L. *J. Chem. Phys.* **1998,** *109*, 10976.

(12) Yang, M. C.; Hwang, C. H.; Kang, H. *J. Chem. Phys.* **1997**, *107*, 2611.

(13) Hwang, C.-H.; Lee, C.-W.; Kang, H.; Kim, C. M. *Surf. Sci.* **2001**, *490*, 144, and references therein.

(14) Shin, T.-H.; Han, S.-J.; Kang, H. *Nucl. Instrum. Methods Phys. Res. B* **1999**, *157*, 191.

(15) Kang, H.; Shin, T.-H.; Park, S.-C.; Kim, I. K.; Han, S.-J. *J. Am. Chem. Soc.* **2000**, *122*, 9842.

(16) Park, S.-C.; Maeng, K.-W.; Pradeep, T.; Kang, H. *Angew. Chem., Int. Ed.* **2001**, *40*, 1497.

(17) Thiel, P. A.; Madey, T. E. *Surf. Sci. Rep.* **1987**, *7*, 211.

(18) Han, S.-J.; Lee, C.-W.; Hwang, C.-H.; Lee, K.-H.; Yang, M. C.; Kang, H. *Bull. Korean Chem. Soc.* **2001**, *22*, 883.

(19) Lahaye, R. J. W. E.; Kang, H. *Surf. Sci.* **2001**, *490*, 144.

(20) Maeng, K.-W. M.Sc. Thesis, Pohang University of Science and Technology, Pohang, South Korea, 2002.

(21) Lahaye, R. J. W. E.; Kang, H. Manuscript in preparation.